TRANSPORT, CHAOS AND PLASMA PHYSICS

Marseille July 5 – 9, 1993

Editors

S. Benkadda
F. Doveil
Y. Elskens

CNRS - Université de Provence
Institut Méditerranéen de Technologie, France

World Scientific
Singapore • New Jersey • London • Hong Kong

Published by

World Scientific Publishing Co. Pte. Ltd.
P O Box 128, Farrer Road, Singapore 9128
USA office: Suite 1B, 1060 Main Street, River Edge, NJ 07661
UK office: 73 Lynton Mead, Totteridge, London N20 8DH

TRANSPORT, CHAOS AND PLASMA PHYSICS

ISBN 981-02-1619-X

Printed in Singapore.

FOREWORD

The International Workshop on *Transport, chaos and plasma physics* was organized at the Mediterranean Institute of Technology (Marseille) from 5th to 9th of July 1993. This meeting made it possible to gather for the first time plasma physicists, dynamical systems physicists and mathematicians, around a general theme focusing on the characterisation of chaotic transport. This workshop was held under the responsibility of

— an international committee composed of R. Balescu (Bruxelles), D. Biskamp (Garching), M. N. Bussac (Ecole Polytechnique, Palaiseau), D. Escande (Tore Supra Group), D. Grésillon (Ecole Polytechnique, Palaiseau), G. Laval (Ecole Polytechnique, Palaiseau), R. S. MacKay (Warwick), V. Rom-Kedar (Weizmann), A. Sen (Ahmedabad) and R. B. White (Princeton).

— an organizing committee with S. Benkadda, F. Doveil, Y. Elskens and X. Garbet (Tore Supra Group).

The organizing committee is pleased to thank Société Française de Physique and the International Association of Mathematical Physics for their sponsorship, the organisations (CNRS – Département des sciences physiques et mathématiques, Université de Provence, C.E.A., Ministère de l'Enseignement supérieur et de la Recherche, Direction de la Recherche et des Etudes Techniques, European Community — Fusion Research Programme, Mairie de Marseille, Conseil Général du département des Bouches-du-Rhône, International Science Foundation) who granted financial support to organise this conference, and Institut Méditerranéen de Technologie for their logistic support.

We also appreciate the dedication of Mrs. Jeanne Durand and Mrs. Patricia Plasse-Fauque to their work, which made it possible to organize this meeting.

Finally, the editors gratefully acknowledge the authors of the enclosed contributions and especially the invited speakers, who willingly took their part in the creative work of writing a timely book.

S. Benkadda, F. Doveil and Y. Elskens

PREFACE

On the front line of key problems still open in the physics of chaos stand the study of chaotic transport and the elaboration of a theory yielding the determination of corresponding transport coefficients. This is the workshop's theme, organised around three questions

— mathematically, in which terms can one describe transport?

— for physicists of thermonuclear fusion, how can one characterise the diffusion of electrons and of their energy in order to produce a coherent theory of so-called anomalous transport?

— what do experimental diagnostics measure, and in which theoretical terms can one interpret them?

The nature of these questions determines the pluridisciplinary spirit of this workshop where participants confronted several results established recently on transport in chaotic (turbulent) media. Besides invited talks and poster sessions, five round tables dealt with the problems above and with the following ones:

— importance and role of coherent structures in transport and their possible presence in tokamaks;

— is turbulence in fusion machines electrostatic or magnetic? There seems indeed to be more evidence for electrostatic turbulence;

— theory and experiment on transport: what does one measure? This round table stressed on indirect experimental measures of transport coefficients and their link to theoretical models;

— mathematical aspects of transport in hamiltonian systems: one mainly discussed the validity of diffusion models for chaotic transport in a framework where it is ill-founded (diffusion in a bounded region of phase space where one cannot separate microscopic and macroscopic scales);

— test particle transport.

It has been very fruitful for both physicists and mathematicians to concentrate on the description and the characterisation of chaotic transport and to focus on the observational effects associated to the transport in magnetic fusion devices. These proceedings, summarizing the lectures and short contributions presented at the workshop, show how the understanding of chaotic transport is not only fundamental for mathematicians of dynamical systems but is a key issue for thermonuclear controlled fusion.

The editors,
S. Benkadda, F. Doveil and Y. Elskens

PARTICIPANTS TO THE INTERNATIONAL WORKSHOP

TRANSPORT, CHAOS & PLASMA PHYSICS

(Marseille, 5-9 July 1993)

1	P	SOSENKO	12	M	OTTAVIANI	23	E	MASCHKE	34	R	RUGGIERI	45	X	GARBET
2	L	GALGANI	13	F	DRISCOLL	24	F	DOVEIL	35	P	KAW	46	F	NGUYEN
3	A	KINGSEP	14	S	BENKADDA	25	P	HENNEQUIN	36	R	POZZOLI	47	D	SHKLYAR
4	A	MONTVAI	15	O	ISHIHARA	26	R	BALESCU	37	G	BACHET	48	P	PLASSE-FAUQUE
5	B	SCOTT	16	M	DUBOIS	27	M	ANTONI	38	A	BERRETTI	49	V	DHYANI
6	J	KALDA	17	V	ROM-KEDAR	28	RS	MACKAY	39	S	RUFFO	50	P	DEVYNCK
7	R	SUDAN	18	FC	SCHÜLLER	29	M	MALAVASI	40	C	SANDOZ	51	A	BECOULET
8	I	DOXAS	19	D	FARINA	30	N	LOPES CARDOZO	41	W	HORTON	52	A	HAMZA
9	L	RUDAKOV	20	G	ZASLAVSKY	31	JL	BOBIN	42	D	BENISTI	53	M	VAN DE WATER
10	D	ROBINSON	21	A	VERGA	32	A	WOOTTON	43	L	CHERIGIER	54	M	DE ROVER
11	A	SAMAIN	22	V	MEL'NIKOV	33	A	HIROSE	44	A	SEN	55	H	MALOVA

CHAPTER 3

DRIFT WAVE TURBULENCE, SELF-ORGANISATION AND INTERMITTENCY

SPACE-TIME STATISTICS OF DRIFT WAVE TURBULENCE WITH COHERENT STRUCTURES

W. HORTON, R.D. BENGTSON,[1] and P.J. MORRISON
Institute for Fusion Studies, The University of Texas at Austin
Austin, Texas 78721 U.S.A.

ABSTRACT

While computer simulations of drift wave turbulence clearly show regimes dominated by coherent vortex structures, the experimental evidence for the existence of such regimes is inconclusive. Two experimental searches on TEXT-U for coherent structures yield mixed results. One study uses a conditional statistical analysis of the plasma fluctuations to select candidate structures and finds no evidence. A second study uses the bispectral analysis to identify phase-correlated structures and finds a structure localized to the $q = 3$ surface.

Motivated by these experiments, we have modeled again the turbulence as a gas of vortices and waves and computed the same conditional potential structures that are reported in the experiments. The physical requirement supposed is that the amplitude of the reference signal exceed a level appropriate for vortex trapping. The important conclusion shown here, which follows from comparison of the computer simulations with the conditional analysis as applied on TEXT-U, is that since the amplitude dependence of the decay rate is sufficiently weak, the conditional averaging method fails to yield conclusions on the presence of the structures. In addition the spatial sampling from the two-probe measurements averaged over a series of discharges may lack the radial resolution needed to identify coherent structures embedded in the background turbulence.

1. Introduction

Plasma structures predicted by hydrodynamic models generally have a preferred direction of wave propagation along the magnetic field and perpendicular to the magnetic field but within the magnetic surface. The numerical simulations of plasma turbulence based on these plasma equations quite generally show the emergence of coherent structures in addition to a spectrum of waves. Here a coherent structure is defined as a region of ordered flows with sufficiently large velocities that the structure has a lifetime appreciably longer than would occur from the corresponding linear dynamics. That is, there is some degree of nonlinear self-focusing or binding. Theory and simulations show that this nonlinear binding occurs when the

[1] Fusion Research Center, The University of Texas at Austin

condition is satisfied,[1-4] that is when the rotation of the fluid around the structure of scale $1/k_\perp$ is faster than the wave dispersion rate $\Delta\omega_{k_\perp}$.

In fluid experiments it is well accepted that anisotropic, inhomogeneous flows contain coherent flow patterns. These patterns are easily seen by visualization techniques for the analogous problem of Rossby waves in sheared flows[5,6] in rotating water tanks. Knowledge of the flow patterns allows detailed predictions of transport.[7] A quantitative measure of these coherent flows has been introduced in the fluid turbulence literature by defining conditional sampling and conditional correlation functions.[8] Certain events in the flow field are used to signal the presence, or possible presence, of the coherent structure. The most common event for the selection procedure is to specify a large amplitude or velocity vector compared with the usual events i.e. those with the root-mean-square amplitude.

Johnsen *et al.*[9] develop the conditional sampling theory, and Pecseli *et al.*[10] and Nielsen *et al.*[11] use the method to find coherent structures in turbulent signals. While Tsui *et al.*[12] have used a bicoherence analysis to find a phase-correlated structure in the edge turbulence of the TEXT tokamak, the conditional statistical sampling method applied by Filippas[13] failed to reveal evidence for a coherent structure. Here we consider the problems associated with the identification of coherent structures in the edge turbulence.

The statistical analysis based on conditional sampling of two-probe time series from variable poloidal spacings and scanned over six radial positions $r = 25.5\,\text{cm}\ [0.5\,\text{cm}]\ 28\,\text{cm}$, which spans the shear flow layer where the plasma velocity changes from -4×10^5 cm/s to $+2 \times 10^5$ cm/s over a 1 cm layer, showed no significant evidence for coherent structures. This null finding of Filippas[13] motivated the present theoretical testing of time series with known components of drift wave-like coherent structures.

In contrast, an independent study by Tsui *et al.*[12] shows significant evidence for coherent structures by sorting probe data according to the radial position with respect to the radial position of the low order magnetic rational surface. Tsui *et al.*[12] use as a measure of coherence the relative strength of the bi-spectrum $\left(\left\langle\varphi(\omega_1)\varphi(\omega_2)\varphi^*(\omega_1+\omega_2)\right\rangle\right.$ appropriately normalized and summed over $0 < \omega_1 + \omega_2 < \omega_{NQ}$) which is shown to reach 80% of its maximum for completely phase-correlated structures. The bi-spectral analysis shows that the coherent feature is localized to within 5−6 mm of the $q(r_s) = 3$ surface.

2. Sampling Conditions

In fluid turbulence where the incompressible velocity vector $\mathbf{v}(\mathbf{x}, t)$ is the primary field the sampling condition is written as

$$E_c = [c \le \mathbf{v}(\mathbf{x}, t) < c + dc] \tag{1}$$

where $\mathbf{c}$ is the velocity vector for the selected event and $d\mathbf{c}$ is the range of neighboring accepted events used to construct a conditional ensemble. In plasma turbulence we use the quasi-2D electrostatic character of the fluctuations and the fact that the electrostatic potential $\varphi(\mathbf{x},t)$ is proportional to the velocity stream function ($\mathbf{v} = \hat{\mathbf{z}} \times \nabla\psi(x,y,t)$ with $\psi = c\varphi/B$) to specify the condition as

$$E_1 = [\varphi_1 \leq \varphi(\mathbf{x},t) \leq \varphi_1 + d\varphi] \ . \qquad (2)$$

Conditions, such as (1) and (2), then create subensemble of $\mathbf{v}(\mathbf{x},t)$ or $\varphi(\mathbf{x},t)$ fields with $\mathbf{v}$ close to $\mathbf{c}$ or φ close to φ_1. Averages of a function F over these subensembles are designated as $\langle F|\mathbf{c}\rangle$ and $\langle F|\varphi_1\rangle$ and are called the conditional average.

Properties of the Selected Subensembles

1. Even when the full velocity field is isotropic, the subensembles generally are not isotropic. According to Adrian[8] one finds that the characteristic eddies selected for example by $|\mathbf{c}| = 1.5\,u$ with $u^2 = \frac{1}{3}\langle \mathbf{v}\cdot\mathbf{v}\rangle$ yields structured flows. Adrian calculates a vortex ring pattern about the given $\mathbf{c}$ vector.

   Adrian defines such structures as "conditional flow patterns" or "conditional eddies" and the term is adopted for plasmas by Johnsen *et al.*[9]

2. Condition E_1 does not presuppose a pattern. When a known signal form is present in the noise the matched signal/noise filter from sonar theory provides an optimal detection in system.

3. The probability densities derived from the number of events satisfying the condition over a range of $\mathbf{c}$ or φ_1 gives a probability density field that occurs in some formulations of turbulence theory. Thus, quantities averaged over conditions $E_\mathbf{c}$ or E_1 can be interpreted directly in those theories.

3. Conditional Statistical Analysis Applied to the 2D Vortex Collision

Here we examine the results of applying the conditional statistical analysis to an example which is dominated by the coherent vortex dynamics when the criterion is visual inspection of isoline dynamics. We take the inelastic dipole-dipole vortex collision reported in Refs. 1 and 2 that yields a final state with a new dipole, a monopole and a spectrum of drift waves. This numerical experiment has been studied by others and is representative of coherent vortex-vortex-wave interactions. We might expect to find a significant amplitude dependence of the nonlinear or conditional correlation functions for these fields. Figure 1 shows the x-y space evolution of the system with details of the numerical experiment given in Ref. 2. We record the voltage signals on an array ($N_y = 43$) of probes along the y (poloidal) direction at $x = 0$ (a given magnetic flux surface).

The signals $\varphi(x = 0, y_k, t)$, $k = 1, 2, \ldots N_y$, are plotted in Fig. 2 with neighboring probe voltages displaced by an appropriate value of $\Delta\varphi$ to give a suitable visualization of the coherent structures in the data files. It is directly evident from this choice of the data display that the fields are dominantly coherent with long lifetimes.

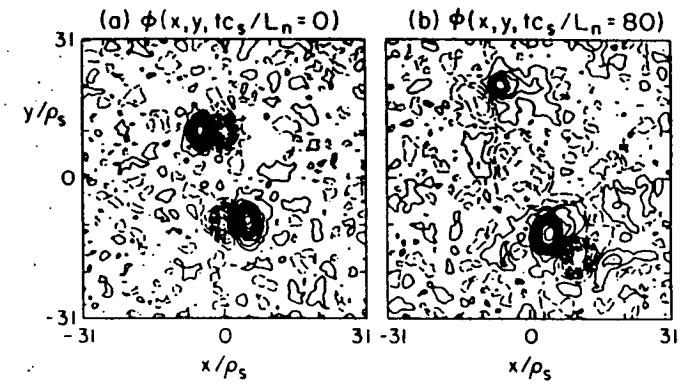

Fig. 1. An inelastic dipole-dipole vortex collision which contains coherent structures with energy $E_v = 23$ and random drift waves with $E_n = 10$. Space-time series are generated from an array of probes along the y-axis at $x = 0$. The contour interval is approximately 5.5 ranging from -55 to +55.

Another example that is a completely analytic synthetic signal is shown in Fig. 3 where a superposition of sech^2-solitary drift waves and a randomly phased broad band wave spectrum are added together. The conditional analysis of this signal, while not discussed, leads to the same conclusions as that given below from the analysis of Figs. 1 and 2.

The probability distribution function for the collision data set is given in Fig. 4. The first several moments are $\bar{\varphi} = -0.252$, $\tilde{\varphi} \equiv \langle(\varphi - \bar{\varphi})^2\rangle^{1/2} = 12.7$, skewness $S = \langle\delta\varphi^3\rangle / \langle\delta\varphi^2\rangle^{3/2} = -0.0539$, and the kurtosis $K = \langle\delta\varphi^4\rangle / \langle\delta\varphi^2\rangle^2 = 8.45$ where $\delta\varphi = \varphi - \bar{\varphi}$. Of course, in this vortex dominated example the statistics deviate appreciably from gaussianity. In the experimental works it is common to select the condition φ_1 in terms of the ratio of the value of φ_1 to the rms $\tilde{\varphi}$ value by defining

$\xi_{\varphi_1} = \varphi_1/\tilde{\varphi}$. For example, Filippas[13] often chooses $\xi_\varphi = \pm 2$ for the condition to study.

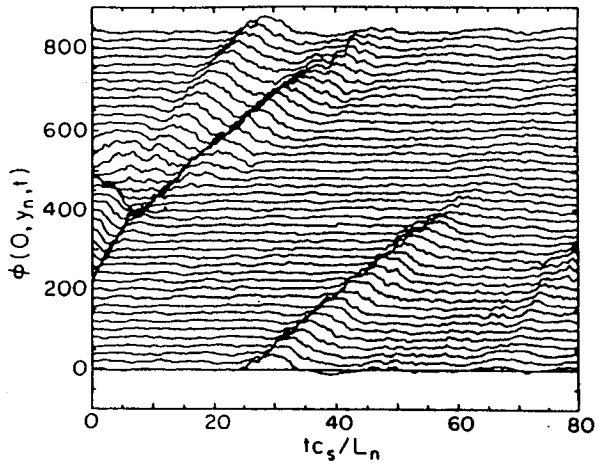

Fig. 2. The space-time display of the voltages recorded at positions $y_n = n\Delta y$, $x = 0$ from the coherent fields in Fig. 1.

Namely, from the amplitude dependence of the lifetimes and propagation velocities derived from the conditionally sampled field there is no evidence to suggest the presence of the solitary waves. Thus, in this sample which has the substantial ratio of signal to noise given by $\langle\varphi^2(S+N)\rangle / \langle\varphi^2(N)\rangle = 1.6/0.4 = 4$ the visual inspection of the multi-probe traces gives a better detection than the conditional decay rate.

Now we show the signals that compose the conditional subensembles choosing the two bins from Fig. 4: one bin which is in the core of the high amplitude vortices and the second bin in the wave region. Namely, we show the subensemble where $\varphi \in [-27, -22]$ which is a bin containing the $\xi_\varphi = -2$ value of φ and the subensemble with $\varphi \in [-5.2, 0.33]$ which has the overwhelming largest number of samples. This small amplitude bin contains all the continuous wave components and has been further analyzed. The bin containing $\varphi_1 = \overline{\varphi} + 2\sigma_\varphi$ has information similar to that in $\overline{\varphi} - 2\sigma_\varphi$

shown in Figs. 5 and 6 and thus is not shown.

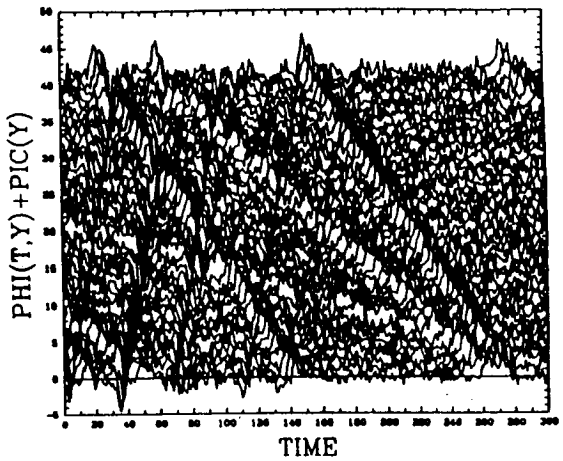

Fig. 3. A synthetic data set displayed as in Fig. 2 created by the superposition of eight randomly distributed sech^2-solitary drift waves and a small amplitude spectrum of randomly phased drift waves. Four of the solitary waves can be detected visually: the spectrum of speeds are $u/v_{de} = \{-0.5, -0.3, -0.1, 1.1, 1.2, 1.3, 1.7, 2.0\}$.

The time-shifted samples from the bin representative of the vortex core voltage $\varphi \in [-27, -22]$ are shown in Fig. 5a. The subensembles averaged signal is shown in Fig. 5b. From Fig. 5a one can see that there are actually two signal types: one with $\partial\varphi/\partial\tau > 0$ and one with $\partial\varphi/\partial\tau < 0$ at this fixed φ-value. If the condition is generalized [Johnsen, *et al.*[9]] to include a positive or negative condition on $\partial\varphi/\partial\tau \cong -v_d\,\partial\varphi/\partial y$ then we find the well-defined pulse shown in Fig. 5b. The pulse is approximately 3/4 the amplitude of the actual structure, about twice as wide and contain substantial wave oscillations that are essentially missing in the coherent structure.

The data analysis of Filippas[13] uses only the condition on φ and replaces the condition on $\partial\varphi/\partial\tau$ with the condition that successive selections be well separated in time. For this large amplitude subensemble the auto-correlation functions are shown in Fig. 6a and the conditionally-averaged correlation function over the subensemble is shown in in Fig. 6b. The first zero crossing point of the correlation function is taken as the measure of the correlation time. The conditionally averaged correlation time

for this conditional potential structure is $\tau_c = (9.4)(L_n/c_s)$.

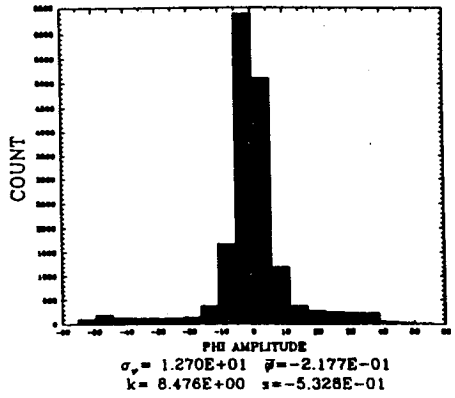

Fig. 4. The probability distribution (pdf) of all samples recorded in Fig. 2. The moments and cumulants (skewnewss and kurtosis) are given. The central portion with $|\xi_\varphi| = |(\varphi - \bar{\varphi})/\tilde{\varphi}| < 1.5$ is gaussian and the vortices produce the small probability tails containing the high amplitude events.

Now we examine the small amplitude (wave components and tails of the vortices) subensemble. Study of the time-displaced set of voltages with $\varphi \in [-5.2, 0.33]$ shows that there are a large number of signals with voltages bounded by $\pm\tilde{\varphi} = \pm 15$ and a relatively few traces with voltages reaching ± 40, which are the solitary wave components "caught by their tails" from the small amplitude condition on φ. A more discriminating set of nonlinear filter conditions would clearly separate these two components.

The same diagnostic information shown in Fig. 5 except selecting the most probable bin from Fig. 4 which has the voltage range $\bar{\varphi} \in [-5.2, 0.33]$ yields a small amplitude oscillatory signal typical of the wave turbulence. The conditional signal for the most probable bin $\langle\varphi|\xi_\varphi = \varphi_c/\tilde{\varphi} = -0.25\rangle$ where $\varphi_c = -2.7$ is the center of the bin.

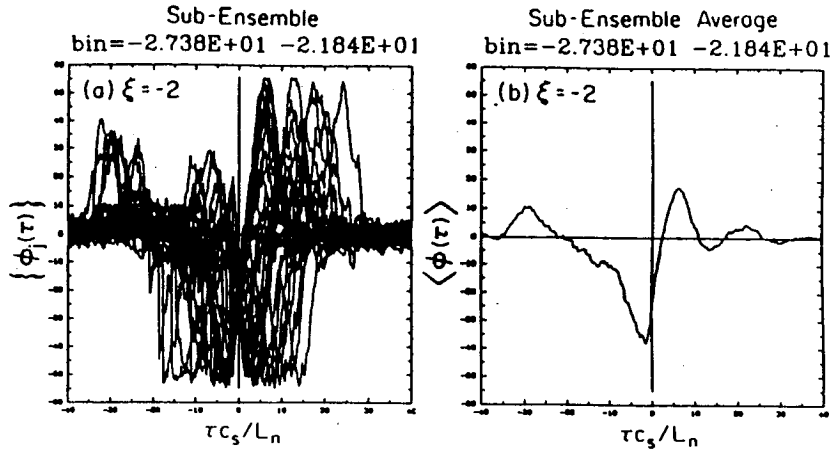

Fig. 5 (a) Members of the subensemble selected by the amplitude condition. The amplitude bin chosen here from Fig. 4 is that containing the $-2\sigma_\varphi$ deviation from $\bar{\varphi}$. (b) the conditional average of signals from part (a) with the condition that $\partial\varphi/\partial\tau > 0$ at $\tau = 0$. The pulse shape in 5(b) is the conditional average pulse $\langle\varphi|\varphi_c = -2\sigma_\varphi, \partial_\tau\varphi > 0\rangle$.

In Fig. 7 we show the individual and subensemble average auto-correlation function obtained from this small amplitude condition. Here the conditional auto-correlation function has its fastest decay rate with the correlation time given by $\tau_c(\bar{\varphi}) = 7.61 L_n/c_s$ for $\bar{\varphi} \in [-5.2, 0.33]$. Comparing this correlation time with that obtained in Fig. 6 we see that this conditional statistical analysis only gives a ratio of $9.4/7.6 = 1.2$ for these qualitatively different parts of the signal. Thus, there is no effective discrimination from this procedure by the use of the conditional correlation time. In another example, as in Fig. 3, some discrimination has been found but the discrimination is weak. The reason for the similarity of these measured characteristic times is (1) that in the high amplitude case the vortex core range is determined by $\rho_s/(1 - v_d/u)^{1/2}$ and (2) in the small amplitude wave regime the dispersion length is determined by $\rho_s/(1 - \omega_*/\omega)^{1/2}$. The diagnostic procedure used here does not effectively discriminate from a rapid drop in the coherent structure from that due to

wave dispersion.

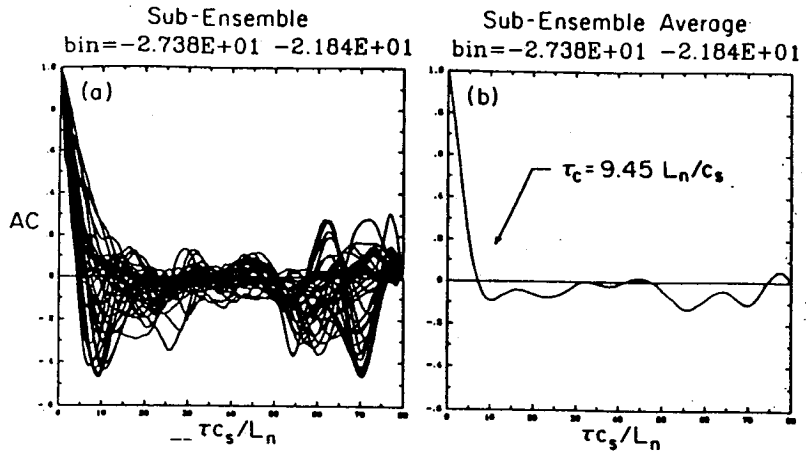

Fig. 6 (a) The auto-correlation function for the conditional subensemble in Fig. 5a. The average of the crossing time $\tau_c = 9.4$ (L_n/c_s) is taken as the measure of the coherence time. (b) The conditional average of the auto-correlation function showing the crossing at 9.4.

Collecting the conditional correlation function data for the ensembles given by the bins in Fig. 4 and following the presentation of Filippas[13] of using the decay rate $\gamma_\tau(\tilde{\varphi}) = 1/\tau_c$ with τ_c defined in Figs. 6 and 7 we show in Fig. 8 the nonlinear decay rate versus the voltage normalized to the rms voltage $\xi = \delta\varphi/\left(\delta\varphi^2\right)^{1/2}$. The decay rate does not show the expected behavior of a fast decay rate (e.g. $\gamma_\tau \geq 0.3$) localized to the small amplitude range $|\sigma_\varphi| < 0.5$ and a relatively slower decay rate for the large $|\xi_\varphi|$ values. Instead, the decay rate $\gamma_\tau(\tilde{\varphi})$ is a relatively constant function with only a weak dependence on the amplitude condition. The same results are found in the analysis of the experimental time series as shown in Fig. 8b taken from Ref. 13.

Additional analysis, not shown here, studies the effective pulse speeds determined by the lags of the maxima of the conditional cross-correlation functions in the space of $\delta y = y_1 - y_2$ and $\tau = t_1 - t_2$ as a function of the amplitude condition $\xi_\varphi = \delta\varphi/\tilde{\varphi}$. This measure of nonlinearity has been used by Pécseli *et al.*[15] for ion holes or BGK structures in ion-ion streaming instabilities with some success. The results for drift waves, however, are not expected to show such a strong amplitude

dependence[3] of the pulse speed.

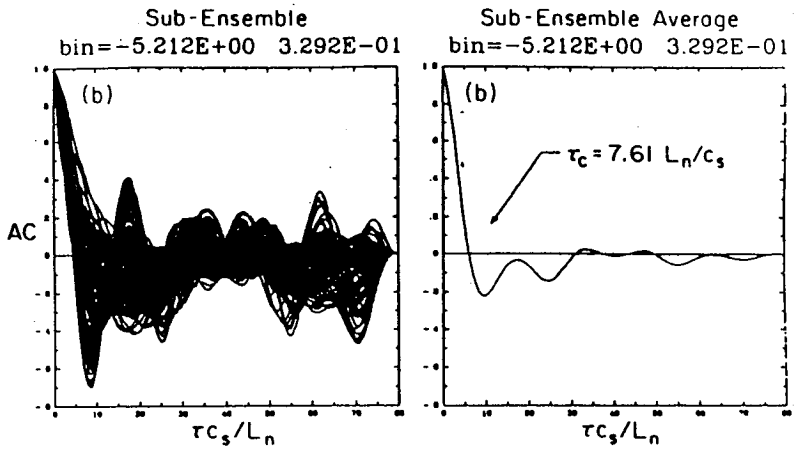

Fig. 7 (a) The auto-correlation function for the conditional small amplitude subensemble in Fig. 5a. The average of the crossing time $\tau_c = 7.6$ (L_n/c_s) is taken as the measure of the coherence time. (b) The conditional average of the auto-correlation function showing the crossing at 7.6.

In conclusion, we see that the variation shown in these nonlinear decay rates defined from conditional correlation functions is relatively modest with $(\gamma_{max} - \gamma_{min})/\gamma_{avg} < 0.1 - 0.2$ for an example in which the flow visualization is obviously coherent in its nature. These results suggest that the conditional statistical analysis applied to the scalar potential or stream function field for drift waves is not a good discriminator for the presence of the coherent structure part of the turbulence field. We suggest that nonlinear filters in the form of neural networks that can be trained to recognize the patterns in these signals should provide a much higher level of discrimination between coherent structures and random wave parts of the turbulent scalar potential. In addition, the use of multiple probe arrays to minimize the unavoidable shot to shot variations should make the proposed vortex patterns clearer. If the vortex structures are localized to the low order rational surface or the shear flow layer, the radial resolution may not be adequate without elaborate compensations for shifts of

the magnetic surfaces from shot-to-shot variations.

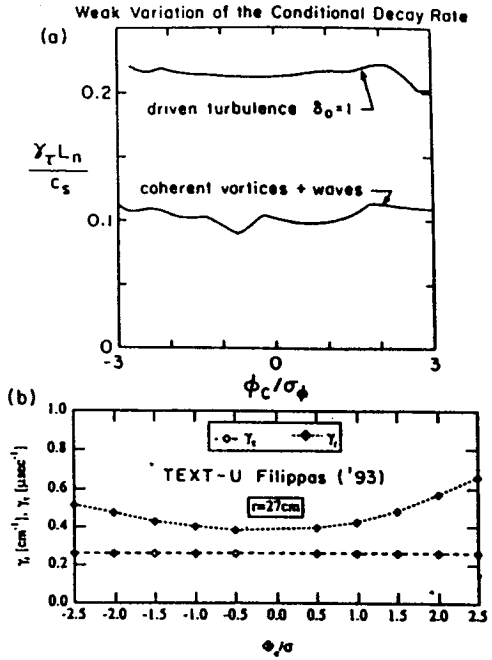

Fig. 8 The decay rate as defined by the reciprocal of the conditional coherence time shown in Figs. 6 and 8 shown as a function of the amplitude condition φ_1 in Eq. (22). The amplitude condition is expressed as a function of $\xi_\varphi = (\varphi - \overline{\varphi})/(\overline{\varphi})$ with values of $|\xi_\varphi| > 3$ discarded as occurring too infrequently to be significant.

Finally, we observe that there remains an important issue to formulate a test statistic declaring the presence of a coherent structure based on the computed variation of the lifetime and/or propagation velocity with the conditional amplitude. Further testing of the null hypothesis, that there is no role (transport, for example) from coherent structures, must be carried out. In the case of sonar messages embedded in noisy signals there is a final test statistic used to declare "FALSE ALARM" when the variations from the detection system are weak.[18] The equivalent test for a role in transport or spectral cascade needs to be formulated for plasma turbulence. Since the "visual" test of the patterns in Figs. 2 and 3 seems to be a more reliable test for the detection of vortices than the amplitude variations found from the conditional sampling, we suggest that neural nets[18] trained to recognize typical vortices together with amplitude measurements may provide a more promising detection system. Sonar signal processing with neural nets has demonstrated impressive results in recognizing different objects.[19]

4. Acknowledgments

The authors thank Drs. Herman Tsui and Vennie Filippas for valuable discussions concerning the search for coherent structures in the TEXT-U data. The work is supported by DE-FG05-80ET-53088.

5. References

1. W. Horton and V. Petviashvili, "On the Trapping Condition for Planetary Vortex Structures," *Research Trends in Physics: Chaotic Dynamics and Transport in Fluids and Plasmas*, eds. W. Horton, Y. Ichikawa, I Prigogine (Ed. in-Chief), G. Zaslavsky, American of Physics (New York, 1993).

2. W. Horton, Phys. Fluids **1** (1989), 524.

3. J.D. Meiss and W. Horton, Phys. Fluids **26** (1983), 990.

4. X.N. Su, W. Horton, and P.J. Morrison, Phys. Fluids B **2** (1990).

5. R.P. Behringer, S.D. Meyers, and H.L. Swinney, Phys. Fluids A **3**, (1991), 1243.

6. M.V. Nezlin, Sov. Phys. Uspekhy **29** (1986), 807.

7. D. Del-Castillo-Negrete and P.J. Morrison, Phys. Fluids A **5**, (1993) 948.

8. R.J. Adrian, Phys. Fluids, **22** (1979), 2065.

9. H. Johnsen, H.L. Pécseli, and J. Trulsen, Plasma Phys. and Controlled Fusion **28** (1986), 1519–1523 and Phys. Fluids **30** (7) (1987), 2239–2254.

10. H.L. Pécseli, J. Juul Rasmussen, and K. Thomsen, Phys. Rev. Lett. **52** (1984) and Plasma Phys. Contr. Fusion **27** (1989), 837.

11. A.N. Nielsen, H.L. Pécseli, and J. Juul Rasmussen, Ann. Geophysicae **10** (1992), 655.

12. H.Y.W. Tsui, K. Rypdal, Ch. P. Ritz, and A.J. Wootton, Phys. Rev. Lett. **12** (1993), 2565.

13. A.V. Filippas, "Conditional Statistical Analysis of Plasma Fluctuations in the Edge of TEXT-U Plasma, FRC Report #433, The University of Texas, 1993.

14. T. Huld, A.H. Nielsen, H.L. Pécseli, and J. Juul Rasmussen, Phys. Fluids B **64** (1990).

15. T. Huld, A.H. Nielsen, H.L. Pécseli, and J. Juul Rasmussen, Phys. Fluids B **3** (7) (1991).

16. H.L. Pécseli and J. Trulsen, Phys. Fluids B **28**, (1989), 1616.

17. V.V. Ol'shevskii, "Statistical Methods in Sonar," (Consultants Bureau, New York, 1978) pp. 147-195.

18. J. Hertz, A. Krogh, and R.G. Palmer, "Introduction to the Theory of Neural Computations," (Addison-Wesley, New York, 1991), Ch. 6.

19. A.J. Maren, D. Jones, and S. Franklin in "Handbook of Neural Computing Applications", Ed. by A.J. Maren, C.T. Harston, and R.M. Pap (Academic Press, New York, 1990) Ch. 15.